coatings

MDPI

Article

Numerical Evaluation of Modified Mortar Coatings for Thermal Protection of Reinforced Concrete and Steel Structures Under Standardized Fire Exposure

Fabrício Longhi Bolina *, Arthur S. Henn, Débora Bretas Silva and Eduardo Cesar Pachla

Department of Sructures, Federal University of Santa Maria (UFSM), Santa Maria 97105-900, Brazil; arthur.henn@acad.ufsm.br (A.S.H.); debora.bretas@ufsm.br (D.B.S.); eduardo.pachla@ufsm.br (E.C.P.)
* Correspondence: fabriciobolina@gmail.com

Abstract

This study investigates the thermal performance of 23 different mortar types, each containing different mixes, properties, and additives. A comprehensive literature review was conducted to collect experimental data on the thermal properties of these mortars, which were then used in a numerical analysis through thermal finite element modeling. The results showed that all mortar types contributed to reducing the internal temperature of structural steel and reinforced concrete elements, with performance primarily influenced by key factors such as the mortar's thermal conductivity, specific heat capacity, thermal diffusivity, and coating thickness. In particular, the mortar with glass fiber reinforced polymer (GFRP) as a slag substitute and the mortar with expanded perlite replacing sand showed the highest thermal protection and achieved a temperature reduction on the order of 100%. In contrast, mortars containing 30% vermiculite or 15% light expanded polyvinyl chloride (PVC) as a sand substitute showed the lowest thermal performance.

Keywords: steel structures; reinforced concrete structures; beams; mortar; fire; structures in fire

check for updates

Academic Editors: Yongcheng Ji and Jun Wang

Received: 26 June 2025
Revised: 7 July 2025
Accepted: 8 July 2025
Published: 9 July 2025

Citation: Bolina, F.L.; Henn, A.S.; Silva, D.B.; Pachla, E.C. Numerical Evaluation of Modified Mortar Coatings for Thermal Protection of Reinforced Concrete and Steel Structures Under Standardized Fire Exposure. *Coatings* **2025**, *15*, 806. https://doi.org/10.3390/coatings15070806

Copyright: © 2025 by the authors. Licensee MDPI, Basel, Switzerland. This article is an open access article distributed under the terms and conditions of the Creative Commons Attribution (CC BY) license (https://creativecommons.org/licenses/by/4.0/).

1. Introduction

Fire resistance in buildings is a fundamental aspect of structural safety, crucial for protecting lives and reducing damage during a fire. The use of fire-resistant materials and specialized construction methods can significantly delay the spread of flames, providing occupants with additional time to evacuate and enhancing the ability of emergency responders to control the fire. Moreover, fire-resistant buildings contribute to economic stability and mitigate environmental impacts by preventing extensive destruction. As urbanization accelerates globally, incorporating fire resistance into building design has become a necessity to ensure the safety and resilience of urban environments. It is imperative that buildings evaluate potential fire hazards and integrate strategies for fire protection, as outlined in standards such as ISO 23932: Fire Safety Engineering—General Principles [1] and ISO 834: Fire Resistance Tests—Elements of Building Construction [2], to enhance the overall fire resilience of the built environment.

Mortar coatings play a crucial role in improving the fire resistance of reinforced concrete and steel structures by acting as a thermal barrier that delays heat transfer during fire exposure. These coatings insulate the underlying materials and help to maintain structural integrity by slowing the temperature rise in steel and concrete, both of which can suffer significant strength loss at high temperatures. For steel structures, where temperatures in

excess of 500 °C can lead to rapid reduction in load-bearing capacity, a protective layer of mortar can significantly extend the time to failure, providing vital time for evacuation and firefighting operations. For reinforced concrete, mortar coatings help to prevent spalling, maintain the bond between steel reinforcement and concrete and reduce the risk of catastrophic collapse. The use of fire-resistant mortar is therefore an important passive fire protection strategy in modern construction and contributes directly to the safety and resilience of buildings. The composition and thermal properties of the mortar play a fundamental role in the extent of the structural fire protection. Some of these mortars (with additives in the mixtures) are described below. Figure 1 shows a case in which fire protection of building structures is carried out using mortar coating.



Figure 1. Thermal protection of steel structures using mortar coatings for fire protection.

Rong et al. (2024) [3] examined the use of Glass Fiber Reinforced Polymers powder (GFRP) as a binder substitute in mixtures with varying proportions of cement, fly ash, and slag. The study observed a decrease in both thermal conductivity and density with increasing GFRP content. Notably, the reduction in thermal conductivity was more pronounced than the decrease in density. These results suggest that GFRP can effectively improve the thermal insulation properties of construction materials, offering a potential alternative for enhancing energy-efficient mortars without significantly altering the material's mass characteristics.

Kouadjo Tchekwagep [4] et al. (2024) investigates the utilization of Chinese Raw Vermiculite (RV) as an alternative to traditional silica sand in mortar formulations made with Calcium Sulfoaluminate (CSA) cement, with the aim of optimizing thermal properties. The study reveals a significant reduction in key thermal parameters, including thermal conductivity, thermal diffusivity, specific heat capacity, and bulk density. These findings suggest that incorporating RV can enhance the thermal insulation performance of CSA-based mortars, providing a potential solution for applications requiring reduced heat transfer and improved energy efficiency.

Topçu et al. (2024) [5] explored the incorporation of sepiolite-based Phase Change Material (PCM) as a replacement for natural sand in mortars (with CaO, SiO_2, Al_2O_3 and Fe_2O_3 as the main chemical composition). The study demonstrated a notable decrease in both thermal conductivity and density. This modification suggests that the use of PCM-impregnated sepiolite can effectively improve the thermal performance of the resulting composites by reducing heat transfer, while also altering the material's overall mass properties. These findings highlight the potential of sepiolite-based PCM systems in enhancing energy-efficient construction solutions.

Zhao et al. (2023) [6] examined the feasibility of using Recycled Carbon Black (RCB) as a substitute for natural sand in mortars. This study appraised the feasibility of recycled carbon black (RCB) derived from scrapped off-the-road (OTR) tires, denoted as RCB-OTR. Their findings revealed a progressive decrease in thermal conductivity, thermal diffusivity, and density as the RCB-OTR content was increased. The incorporation of RCB-OTR into mortars remarkably influenced their thermal properties. The oven-dry thermal conductivity of mortars dropped from 1.800 to 0.272 W/m.K when RCB-OTR replaced 100% of fine aggregates. Under the same aggregate replacement ratio, the volumetric heat capacity dropped from 1.438 to 1.044 MJ/m^3K, and the thermal diffusivity dropped from 1.255 to 0.263 mm^2/s. This reduction in thermal parameters indicates that RCB can contribute to the production of materials with improved insulating properties, presenting an environmentally friendly alternative for enhancing the thermal performance of construction composites.

El Boukhari et al. (2023) [7] investigated the potential of using Olive Solid Waste (OSW) as a replacement for sand in mortar mixtures. The study demonstrated a decrease in density, thermal conductivity, and thermal diffusivity as the proportion of OSW in the mixture increased. These results indicate that OSW can be effectively utilized to reduce the thermal transfer properties of mortars, offering a sustainable alternative that not only enhances the thermal performance but also promotes waste valorization in construction applications.

Adediran et al. (2023) [8] proposed the incorporation of Ladle Slag (LS) and Blast Furnace Slag (BFS) as partial substitutes to enhance Fayalite Slag (FS)-based mortars. The study found that the substitution of FS with BFS and LS led to an increase in thermal conductivity, compared to mortars composed solely of FS. This indicates that while the use of BFS and LS can modify the thermal behavior of the mortar, it may also contribute to a higher heat transfer rate, potentially influencing the material's suitability for applications requiring lower thermal conductivity.

Asadi et al. (2025) [9] explored the use of Micronal 24D, a Microencapsulated Phase Change Material (MPCM, with the chemicals composition 17–24% SiO_2, 4–7% Al_2O_3, 1.5–5% Fe_2O_3, 60–67% CaO, 1–5% MgO, 1.5–3% SO_3, and 0.2–1.5% $K_2O + N_2O$), added in a fixed proportion to cement content in mortars. The study found that, with the inclusion of MPCM, there was a reduction in both thermal conductivity and density, regardless of the cement content. This suggests that the presence of MPCM can significantly enhance the thermal insulation properties of mortars, offering an effective solution for improving energy efficiency while maintaining flexibility in cement composition.

Karakaş et al. (2023) [10] investigated the use of Expanded Perlite (EP) and Raw Perlite (RP) as substitutes for natural sand in mortars with fly ash as the binder. The study revealed that the mortar mix with EP as a complete replacement for sand exhibited significant reductions in both thermal conductivity and density compared to the mix with RP as a total sand substitute. This suggests that EP has greater potential to enhance thermal performance and reduce the weight of mortars, making it a more effective alternative for applications requiring improved thermal insulation properties.

Salem et al. (2020) [11] investigated the potential of using Vegetable Synthetic Sponge (VSS) as a replacement for natural sand in mortar mixes. The results demonstrated that as the proportion of VSS increased, there was a corresponding decrease in thermal conductivity, thermal diffusivity, and density. These outcomes suggest that VSS can effectively reduce the thermal transfer properties of the material, offering a promising eco-friendly alternative for improving the thermal performance of mortars.

Latroch et al. (2018) [12] explored the use of Expanded Polyvinyl Chloride (EPVC) as a substitute for natural sand in mortar mixes. Their findings revealed that increasing the proportion of EPVC resulted in a decrease in thermal conductivity and density. These results

highlight EPVC's potential as an effective material for enhancing the thermal insulation properties of mortars.

In this paper, the thermal performance of a variety of mortars used as thermal protection for beams in case of fire is investigated. A total of four beams (two of reinforced concrete and two of steel, with different geometries) were investigated to understand the influence on the cross-sectional temperature. A total of 23 mortars with different mixtures were tested. The aim of this research is to understand what type of mortar, what mix and what additives need to be added to the mortars to improve the thermal behavior of structures in case of fire. Mortar thicknesses of 10, 20 and 30 mm were considered.

2. Materials and Methods

2.1. Mortar Characteristics, Parameters and Nomenclatures

As shown in Table 1, Various mortar mix designs were analyzed, each incorporating different materials as partial or full replacements for conventional components. For detailed information on the experimental procedures used in each study (specimens' dimensions, experimental criteria, standardized procedure assumed), readers are encouraged to consult the original references cited in this paper.

The reference mortar mix, denoted as M1, consists of cement, sand, and water, serving as the baseline for comparative analysis. Several alternative mixes were developed by introducing supplementary materials to replace cement, sand, or slag, with a focus on enhancing thermal performance characteristics.

The M2 mix utilizes 16% fly ash and 4% Glass Fiber Reinforced Polymer (GFRP) powder as a partial replacement for cement, while M3 employs the same proportions of fly ash and GFRP powder but substitutes slag instead. Further exploring the use of GFRP, M4 replaces 40% of slag with GFRP powder, and M5 incorporates a 40% replacement of cement with GFRP powder. Additionally, M6 combines 20% fly ash and 40% GFRP powder as a dual replacement for cement, demonstrating the versatility of these supplementary materials.

To assess the impact of raw vermiculite (RV) on mortar properties, M7 and M8 replace 30% and 100% of silica sand, respectively, with RV. These mixes also incorporate calcium sulfoaluminate (CSA) cement. Phase Change Materials (PCM) were also examined, with M9 and M10 substituting 20% and 40% of sand with PCM, respectively, to explore their thermal regulation potential.

Recycled Carbon Black (RCB) was integrated into the mixes as sand replacement, with M11 and M12 featuring RCB substitution rates of 30% and 100%, respectively. Similarly, Olive Solid Waste (OSW) was tested for its viability as a sand alternative, with M13 and M14 incorporating OSW at replacement rates of 5% and 15%.

Microencapsulated Phase Change Materials (MPCM) were also explored through M15, M16, and M17, each adding Micronal 24D—a commercial MPCM—at a consistent rate of 20% by cement weight, with variations in cement content. Additionally, the study examined the use of lightweight aggregates, with M18 and M19 fully replacing sand with Expanded Perlite (EP) and Raw Perlite (RP), respectively.

Finally, innovative organic and synthetic materials were incorporated into the mortar designs. M20 and M21 introduced Vegetable Synthetic Sponge (VSS) as a sand replacement at levels of 5% and 20%, while M22 and M23 utilized Expanded Polyvinyl Chloride (EPVC) aggregates to replace a sand mix composed of 60% quarry sand and 40% sea sand. These diverse mortar formulations highlight the potential of alternative materials to enhance thermal performance

Table 1 shows the description of the individual mortars and the respective name, as well as the reference in which the parametric data of these mortars are contained. Appendix A describes the mixtures of the individual mortars in detail. These parametric

data are listed in Table 2, in particular the thermal conductivity and the density of each mortar, which are linked to the thermal diffusivity of the thermal model. There is a gap in the definition of specific heat in these references. In this sense, a specific heat of 1.0 kJ/kg·K was used as the standard in all cases.

Table 1. Mortar cases and nomenclatures.

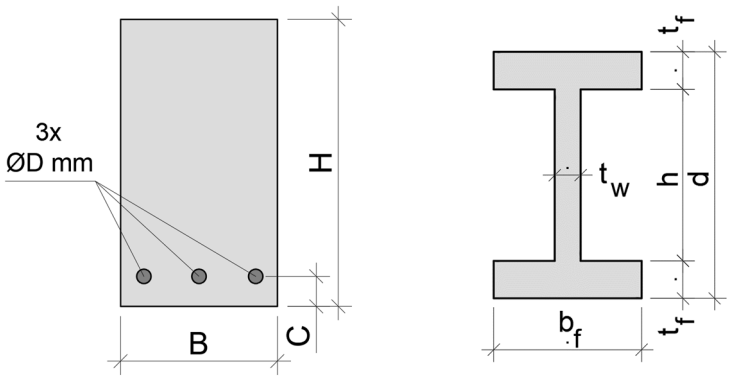
Mortar Name	Description	Reference
M1	Conventional mortar with cement and sand	Rong et al., 2024 [3]
M2	4% Glass Fiber Reinforced Polymers Powder and 16% Fly Ash cement replacement	
M3	4% Glass Fiber Reinforced Polymers Powder and 16% Fly Ash Slag replacement	
M4	40% Glass Fiber Reinforced Polymers Powder Slag replacement	
M5	40% Glass Fiber Reinforced Polymers Powder Cement replacement	
M6	40% Glass Fiber Reinforced Polymers Powder and 20% Fly Ash cement replacement	
M7	Raw Vermiculite 30% sand replacement	Tchekwagep et al., 2024 [4]
M8	Raw Vermiculite 100% sand replacement	
M9	Phase Change Material 20% sand replacement	Topçu et al., 2024 [5]
M10	Phase Change Material 40% sand replacement	
M11	Carbon Black 30% sand replacement	Zhao et al., 2023 [6]
M12	Carbon Black 100% sand replacement	
M13	Olive Solid Waste 5% sand replacement	EL boukhari et al., 2023 [7]
M14	Olive Solid Waste 15% sand replacement	
M15	Microencapsulated Phase Change Materials 20% cement weight addition	Asadi et al., 2025 [9]
M16	Microencapsulated Phase Change Materials 20% cement weight addition	
M17	Microencapsulated Phase Change Materials 20% cement weight addition	
M18	Expanded Perlite 100% Sand replacement	Karakaş et al., 2023 [10]
M19	Raw Perlite 100% Sand replacement	
M20	Vegetable Synthetic Sponge 5% sand replacement	Salem et al., 2020 [11]
M21	Vegetable Synthetic Sponge 20% sand replacement	
M22	lightweight aggregates of Expanded Polyvinyl Chloride 15% sand replacement	Latroch et al., 2018 [12]
M23	lightweight aggregates of Expanded Polyvinyl Chloride 75% sand replacement	

Table 2. Thermal properties of the mortar cases.

Mortar Name	Thermal Conductivity (W/mK)	Density (Kg/m^3)
M1	0.86	1900
M2	0.39	1850
M3	0.3	1870
M4	0.14	1700
M5	0.28	1500
M6	0.25	1600
M7	1.75	2100
M8	0.8	1830
M9	0.891	1471
M10	0.674	1240
M11	1.094	1779
M12	0.272	1058
M13	0.87	1750
M14	0.58	1375
M15	0.8	1767.8
M16	0.9	1894.6
M17	0.8	1956.9
M18	0.19	880
M19	0.48	1760
M20	0.769	1610
M21	0.368	1170
M22	1.4	1750
M23	0.76	1250

2.2. Beams Cross-Sectional Geometries

A total of four cases of beams were tested: two for reinforced concrete beams and two for steel beams. The difference between the two is the cross-section dimensions. The cross-section types are shown in Figure 2 and the geometric data in Tables 3 and 4 for reinforced concrete and steel cases, respectively.



(**a**) Reinforced concrete beam (**b**) Steel beam

Figure 2. Cross-sectional data of the beams.

Table 3. Reinforced concrete beams nomenclature.

Beam Name	*B*	*H*
Bc1	150 mm	500 mm
Bc2	250 mm	500 mm

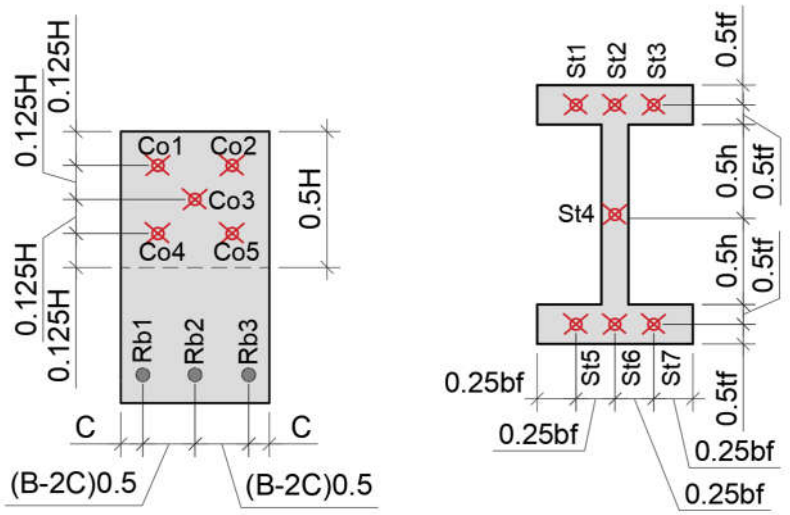
Table 4. Steel beams nomenclature.

Beam Name	d	b_f	t_f	h	t_w
Bs1	229	210	23.7	180	14.5
Bs2	535	166	16.5	502	10.3

In the concrete beam, B denotes the beam width, H the beam height, and C the thickness of the reinforcement cover. For the steel profile, bf represents the flange width, *tf* the flange thickness, h the web height, t_w the web thickness, and d the total section height.

2.3. Control Points

The average temperature in each cross-section was determined by specific points in the cross-section of the beams. For the reinforced concrete beams, the temperature was measured at the points used to determine the bending moment capacity of these structures by analytical methods, i.e., in the area of the concrete above the neutral axis and the positive reinforcement. In this sense, for the RC beams, the average temperature in the concrete was taken as control points Co1 to Co5 and the average temperature in the rebars as control points Rb1 to Rb3, as shown in Figure 3a. In the case of the steel profile, the average temperature was that defined by control points St1 to St7, as shown in Figure 3b.



(**a**) Reinforced concrete beam (**b**) Steel beam

Figure 3. Control points assumed in the average temperature of the beam cases.

2.4. Finite Element Modeling

The presented study is based on a thermal analysis solved with the software Abaqus [13]. Equation (1) shows the governing equations used to define the temperature field and transfer in the cross-sections. The thermal diffusivity is based on the mass loss ρ, the thermal conductivity λ and the specific heat C_p. The parameters of the individual mortars have already been listed in Table 2. For the concrete, reinforcement and steel, which were assumed as the base material of the beams, all parameters correspond to those proposed in Eurocode [14].

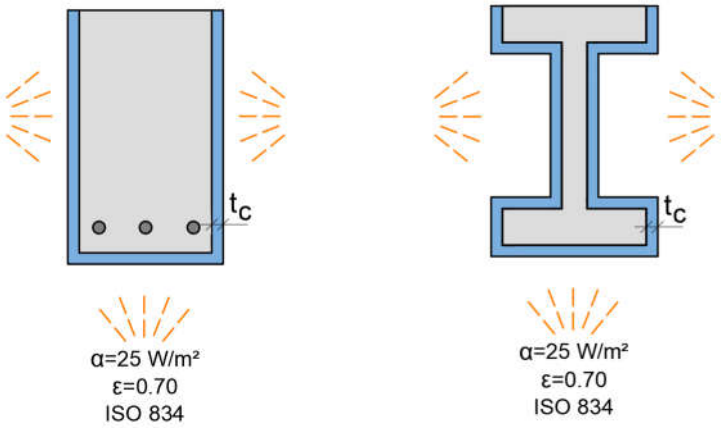
$$\alpha = \frac{\lambda}{\rho . C_p} \quad (1)$$

Equation (2) defines the governing equation for convective and radiative heat transfer process [15], where n_y and n_z are the vector components of the outward perpendicular to the cross-sectional area; h_{rad} and h_{con} are the radiative and convective heat transfer

coefficients, respectively; T is the ambient temperature (assumed as 20 °C) and T_E is the temperature of the environment subjected to fire (considered as ISO 834 standardized time-temperature, as proposed by EN 1992-1.2 [14] to structural design in case of fire, similar to ASTM E119 [16]). The radiation heat transfer coefficient is given by Equation (3), where σ is the Stefan-Boltzmann constant ($\sigma = 5.67 \times 10^{-8}$ W/m^2.°C^4), and ε the emissivity factor (assumed as 0.70 according to EN 1992-1.2 [14]). As shown in Figure 4, the convective heat transfer was 25 and 9 W/m^2 °C on the surface exposed to the fire and the unexposed surface respectively. Heating was applied to the bottom surface of the beam, as is common in residential buildings exposed to internal fires.

$$k \cdot \left(\frac{dT}{dy} \cdot n_y + \frac{dT}{dz} \cdot n_z \right) = -(h_{rad} + h_{con}) \cdot (T - T_E) \quad (2)$$

$$h_{rad} = 4 \cdot \sigma \cdot \varepsilon \cdot \left(T^2 + T_E^2 \right) \cdot (T + T_E) \quad (3)$$



(**a**) Reinforced concrete beam (**b**) Steel beam

Figure 4. Heating process and parameters of the assumed beam cross-sections.

The problem is solved using a 3D model and a non-linear thermal transient analysis. The Abaqus library was used to represent the concrete as a finite element DC3D8 with classical integration. The mesh is quite fine-meshed with a size of 1.0 mm × 1.0 mm × 1.0 mm. A convergence criterion of 0.1°C and a time increment of 0.001s was used.

The criteria and procedure for the FE model (finite elements, mesh size, mesh validation, steps, boundary conditions, governing equations, etc.) were validated by the authors through an extensive full-scale experimental test. Some of these results and criteria can be found in [17–19]. The numerical simulation is also based on the approaches presented by the authors in [20].

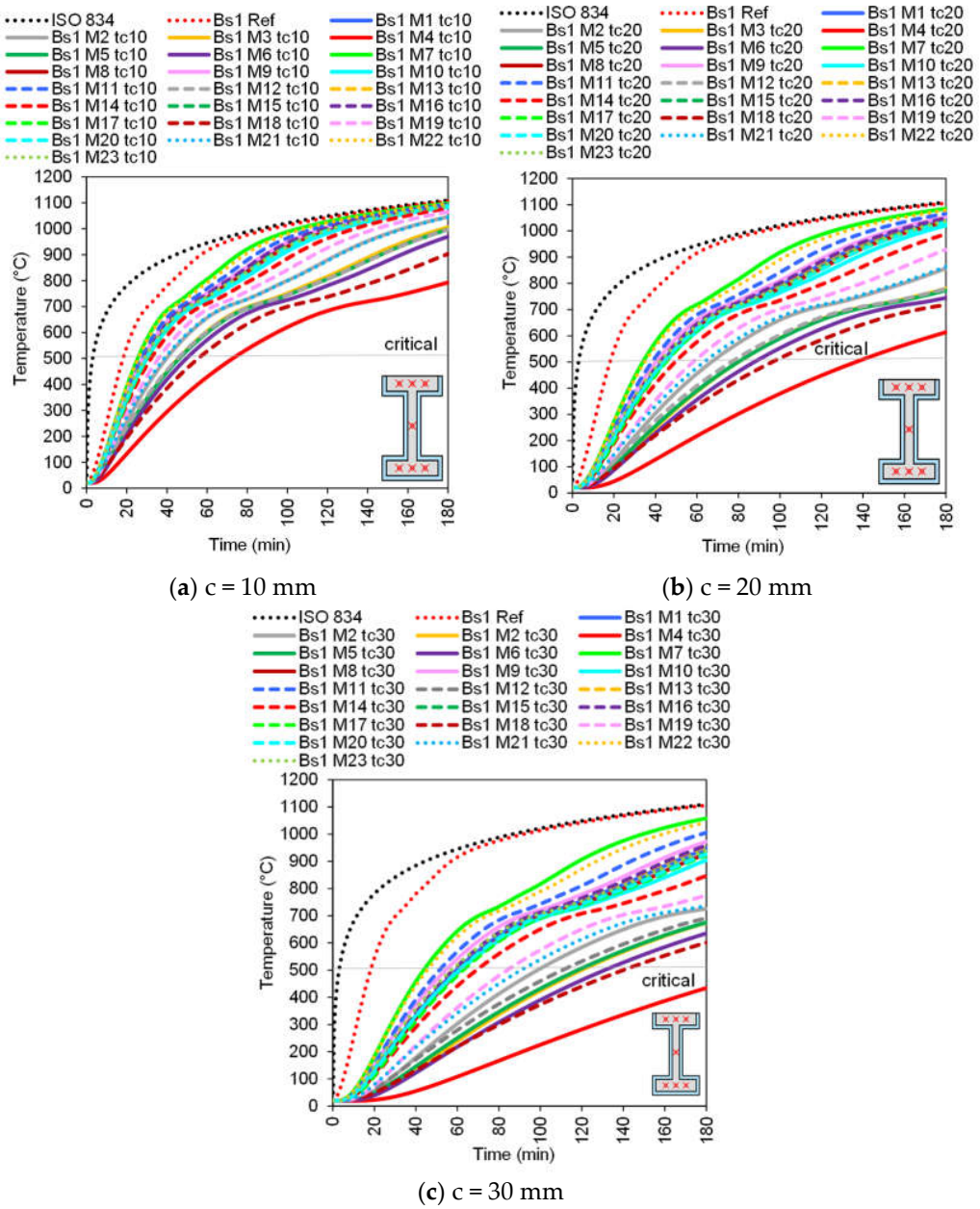
It should be emphasized that in all cases the detachment of the mortar during the period of fire exposure was not taken into account. It was assumed that the mortar remains in contact with the cross-section for the entire duration of the fire under consideration. The detachment of the mortar in the event of fire needs to be further investigated and further research in this direction is required.

3. Results

The results for beam cases Bs1, Bs2, Bc1, and Bc2 are presented and discussed in detail in the following section, focusing on the influence of different mortar types and thicknesses on the temperature distribution within steel and concrete structural elements. The analysis highlights how each configuration affects thermal insulation performance, peak temperature values, and time to reach critical temperature thresholds under fire exposure.

3.1. Bs1 Beams

The average temperature of the steel cross-section is shown in the Figure 5a–c for mortar thickness 10 to 30 mm, respectively.



(**a**) c = 10 mm (**b**) c = 20 mm

(**c**) c = 30 mm

Figure 5. Cross-section temperature in the Bs1 beams.

Firstly, it is important to emphasize that none of the mortars protected the steel from reaching the critical temperature leading to mechanical degradation, with the exception of M4 with a thickness of C = 30 mm, which proved to be the most effective case. M18 was the second case that showed the best thermal performance but does not prevent the steel from reaching the critical temperature regardless of the assumed thickness. M7 and M22 have a very similar performance and both proved to be the worst mortars to protect the steel beams from the fire.

M4 proves to be the most effective solution for protecting steel structures against the effects of fire. With an M4 thickness of 10 mm, the average temperature of the profile is reduced by 69.4, 53.0, 42.1, 34.6, 32.1 and 28.3% compared to a beam without thermal protection (ref) at 30, 60, 90, 120, 150 and 180 min of fire duration. If the thickness is

increased to 20 mm, the average temperature of the profile decreases by 87.6, 76.0, 65.7, 57.0, 50.0 and 44.5% during these times. If the thickness is increased to 30 mm, the average temperature of the steel profile drops by 95.0, 87.6, 79.8, 72.5, 66.0 and 60.7% in the same times. As shown, the M4 mortar can reduce the average temperature of the steel profile by up to 98.9% compared to the unprotected case, depending on the thickness of the mortar layer and the duration of fire exposure.

Although M18 does not prevent the profile from reaching its critical temperature, this mortar has shown good performance and can be considered an effective solution to protect steel structures from fire. The performance of M18 is very similar to that of M6 and can be considered equivalent. As noted in the previous case, the mortar is most effective in the third 30 min and reduces its thermal influence at the end of the test, i.e., at 180 min. With a mortar thickness of 10 mm, the reduction in the average temperature of the profile at 30 min of ISO fire is 58.1%, but decreases to 18.3% at the end of the fire program. If the mortar thickness is increased to 20 mm, the thermal protection improves significantly, by 77.4 and 35.1% compared to the "Ref" case at 30 and 180 min respectively. The same applies to a thickness of 30 mm, which reduces the average temperature of the profile by 87.4, 75.5, 65.7, 57.4, 50.7 and 45.6% for a fire duration of 30, 60, 90, 120, 150 and 180 min respectively.

Regarding the M7 and M22 cases, their thermal protection was minimal compared to the other cases. Both showed a very similar performance and can be considered as an equivalent solution. Assuming a thickness of 10 mm, their reduction in the average temperature of the profile was 19.0, 13.0, 4.0, 2.0, 1.0 and 0.0% at 30, 60, 90, 120, 150 and 180 min of fire exposure. As can be seen, this mortar can produce the same temperature of the profile without thermal protection. When the thickness is improved to 20 mm, the reduction of the average temperatures is around 38.3, 22.8, 15.4, 6.9, 3.6 and 2.4 % at the same times. Improving to 30 mm, the reduction at 30, 60, 90, 120, 150 and 180 min of fire expo-sure was 54.5, 31.3, 24.6, 16.4, 9.4 and 5.7 lower in relation to the reference.

For the M4 mortar, the maximum temperature to which the profile was exposed was 793.1, 613.4 and 434.6 °C when the mortar thickness was 10, 20 and 30 mm respectively. In the case of M18, the maximum temperature was 903.1, 717.3 and 601.4 °C for mortar thicknesses of 10, 20 and 30 mm, respectively. For the M7 thickness, the maximum temperature was 1098.3, 1085.5 and 1058.7 for the same thickness, which shows that the profiles reach more than 1000 °C even at C = 30 mm. The same applies to the M22, for which the maximum temperature at 10, 20 and 30 mm mortar thickness was 1096.7, 1079.8 and 1042.9 °C.

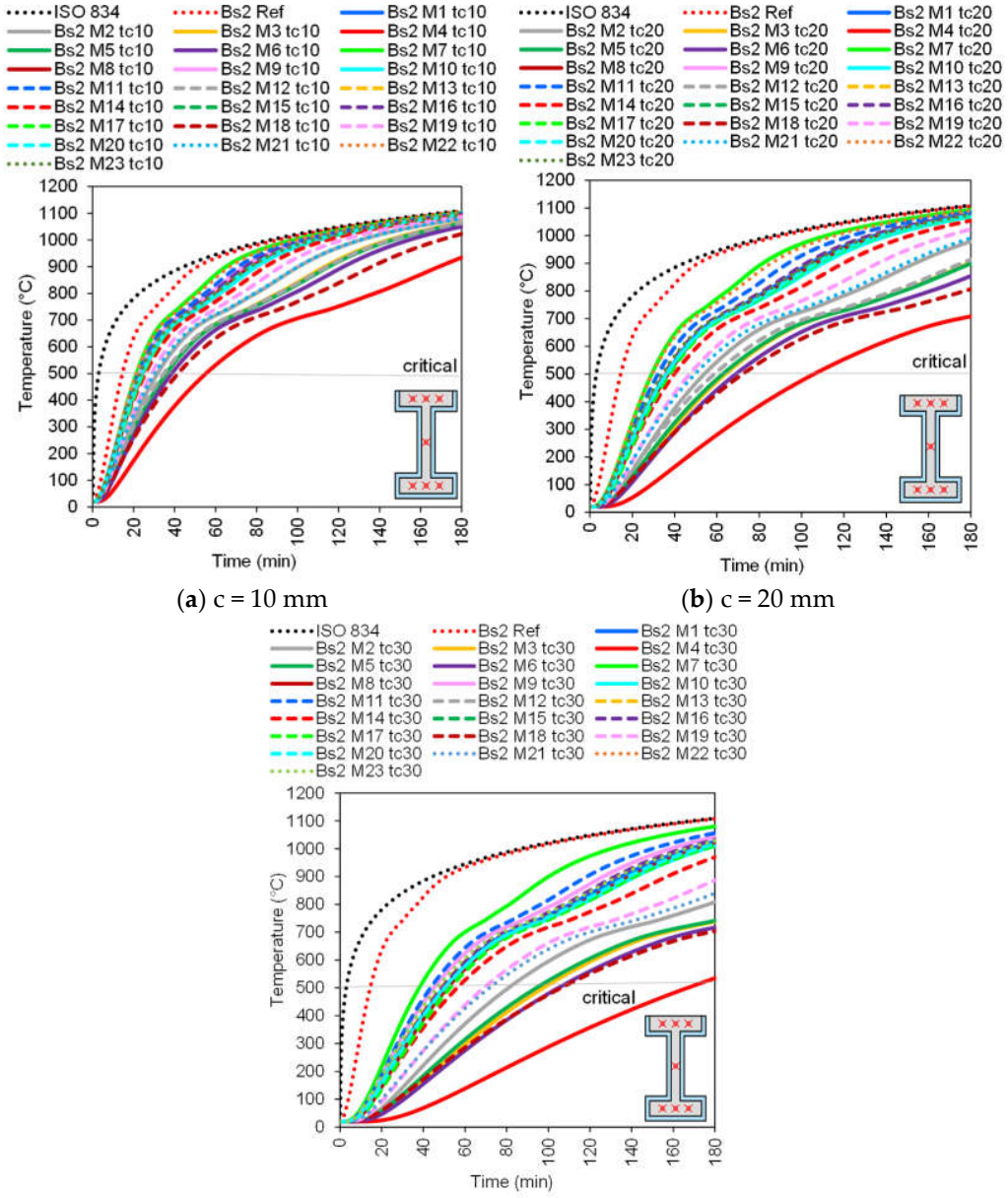
3.2. Bs2 Beams

The average temperature of the steel cross-section is shown in the Figure 6a–c for mortar thickness 10 to 30 mm, respectively.

Contrary to the prior example, the Bs1, none of the mortars assumed in the analysis were apt to prevent the profile from reaching the critical temperature. M4 maintains their remarkable thermal competency, but do not avoid the crucial temperature. However, the time in which the M4 with C = 30 mm exceeded the critical temperature was 173 min.

This results also highlight the influence of the cross-section in this analysis, or also the shape of the cross-section [21]. The phenomenon is generally known as the "section factor" and is critical in establishing how a steel section's shape impacts its temperature rise during fire exposure. The shape factor is the ratio of the heated perimeter to the cross-sectional area of the profile. The cross-section factor influences the rate at which steel heats up in a fire. A higher cross-section factor (i.e., more exposed area in ratio to the steel mass) results in faster heating and thus higher temperatures in a shorter time. This is of critical importance

in fire engineering, but it will not be addressed in this research because it is not the subject of the suggested analysis.



(**a**) c = 10 mm (**b**) c = 20 mm

(c) c = 30 mm

Figure 6. Cross-section temperature in the Bs2 beams.

With an M4 thickness of 10 mm, the temperature reduction compared to the reference beam ("ref", i.e., the beam without mortar to be protected) is 61.3, 43.2, 31.8, 27.8, 22.1 and 15.6% at 30, 60, 90, 120, 150 and 180 min ISO 834 exposure respectively. When improving to 20 mm, the reduction is 85.7, 69.5, 57.1, 47.4, 40.3 and 36.0% at 30, 60, 90, 120, 150 and 180 min ISO 834 respectively. At a mortar thickness of 30 mm, the reduction is 94.6, 85.2, 74.9, 65.8, 58.1 and 51.7% at the same time. As can be seen, the M4 mortar can reduce the average temperature of the profile by almost 100%, depending on the thickness and fire duration.

As discussed for M4, the M18 and M6 mortars also exhibit interesting fire behavior, developing a very similar performance between them and showing a behavior slightly inferior to that of M4, and must be highlighted as an interesting solution. At a thickness of 10 mm, the reduction in the average temperature of the profile was 48.7, 32.7, 26.4, 19.9, 12.3

and 7.6% lower than that of the reference profile at 30, 60, 90, 120, 150 and 180 min. When the thickness was increased to 20 mm, the temperature reduction was 77.4, 64.2, 52.6, 44.1, 38.1 and 35.1% at the same times. Increasing the thickness reduces the average temperature and the temperatures decrease by 85.4, 69.1, 56.7, 47.3, 40.5 and 36.4% at the same ISO 834 standardized times.

On the other hand, cases M7 and M22 also show the worst behavior compared to the other cases. It can be assumed that the reduction in the average temperature of the profile is minimal compared to the reference beam. Assuming a thickness of 10 mm, the reduction in average temperature was 13.4, 8.3, 1.9, 1.0, 0.7 and 0.6% at 30, 60, 90, 120, 150 and 180 min of exposure to the ISO 834 fire. With an improvement to 20 mm at the same standardized times, the average temperature decreases by 30.7, 18.6, 8.5, 3.5, 2.1 and 1.4%. With a mortar thickness of 30 mm, the temperature drops by 48.2, 26.7, 17.9, 8.2, 4.5 and 3.0% compared to the reference beam at the same ISO 834 times. Even with the worst performance, it can be seen that the protection level reaches a maximum of almost 50.0% of the temperature reduction during the initial fire exposure (i.e., 30 min), but a maximum of 3.0% at the end (i.e., 180 min). The degree of the thermal behavior of the mortar reduces with the improvement of the temperature.

For mortar M4, the maximum temperature to which the profile was exposed was 934.7, 708.2 and 534.9 °C, for mortar thicknesses of 10, 20 and 30 mm respectively. In cases M7 and M22, the maximum temperature reached by the profile was 1100.8, 1091.4 and 1074.0 °C for mortar thicknesses of 10, 20 and 30 mm respectively. The temperature difference between the best and worst cases is approximately 200, 300 and 500 °C at 10, 20 and 30 mm respectively. This shows that the nature of the mortar can influence the average temperature of the cross-section of structures exposed to fire and must be taken into account in structural design. The significant temperature variations caused by different mortar types and thicknesses can alter the mechanical properties of structural materials, potentially affecting structural integrity and fire resistance classification. Therefore, thermal protection selection should be carefully considered in structural design, and further coupled thermo-mechanical analyses are recommended to evaluate these effects comprehensively.

3.3. Bc1 Beams

3.3.1. Average Temperature in the Concrete

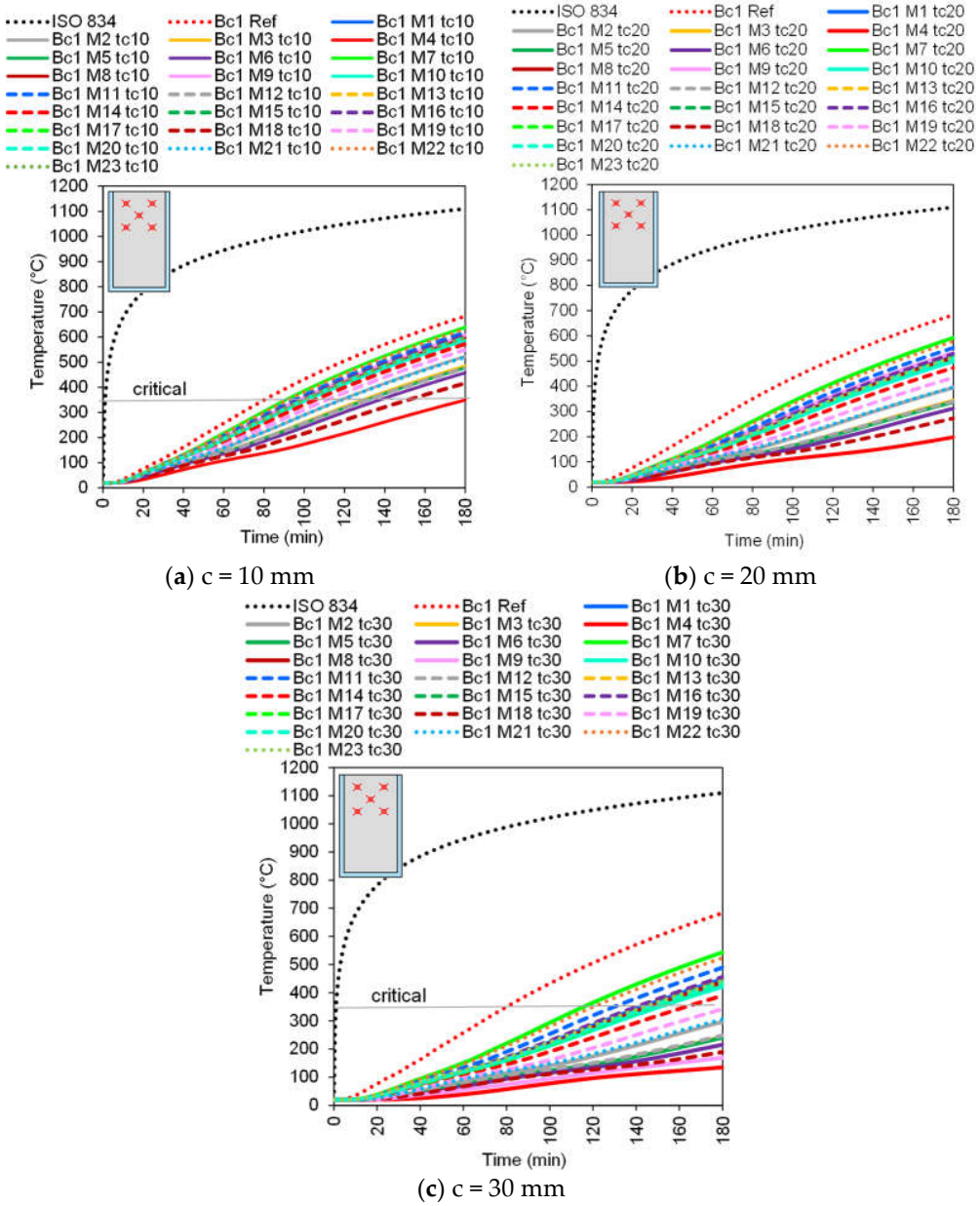
The average temperature of the concrete part of the cross-section is shown in the Figure 7a–c for mortar thickness 10 to 30 mm, respectively.

It is important to emphasize that a mortar thickness of 10 mm is already sufficient to protect the beams from cross-sectional heating. The degree of protection obviously depends on the mortar mix, and the additives used play an important role in the performance of structures exposed to fire. Mortars are a solution to be considered in structural fire design, even for RC structures.

As observed in all cases, M4 showed the best performance compared to all other cases. This was also observed in the steel structures described in the previous section. M4 reduces the temperature in the concrete cross-sectional area (used to define the bending moment in the analytical design) by 52.9, 57.2, 60.7, 57.1, 52.5 and 48.8% in the ISO 834 times of 30, 60, 90, 120, 150 and 180 min, respectively, when the mortar thickness is 10 mm. If the thickness is increased to 20 mm, the results improve to 74.6, 73.2, 73.3, 74.0, 73.2 and 71.0% in the same times. With a mortar thickness of 30 mm, the extent of the decrease improves to 81.5, 84.3, 82.3, 80.6, 80.3 and 80.3% compared to the design without thermal protection at the same times of the standardized fire.

M18 also showed the best performance, as described for the steel structures. However, its performance was significantly lower than that of M14 and should be considered a good

mortar for the protection of these structures. At a mortar thickness of 10 mm, the average temperature of the concrete in the cross-section of the beam decreases by an average of 45.0%. At a mortar thickness of 20 mm, the temperature decreases by 65.0%, and at a mortar thickness of 30 mm, the average temperature in the cross-section decreases to 74.0%. In this case, M6 shows a similar performance and a very similar level of thermal protection and can also be considered a good mortar to be taken into account in the fire design of reinforced concrete structures.



(**a**) c = 10 mm (**b**) c = 20 mm

(**c**) c = 30 mm

Figure 7. Cross-section temperature in the concrete part in the case of Bc1 beams.

In the range of the worst mortar coating materials, M7 and M22 showed an uninteresting level of thermal protection for these structures. Almost both reduce the temperature of the cross-section compared to the reference beam (without thermal protection), but their performance was worse compared to all other mortar coatings. At 10 mm thickness, these mortars show on average a reduction in the order of 15.4, 15.8, 12.6, 10.0, 8.5 and 7.6% compared to the reference beam at 30, 60, 90, 120, 150 and 180 min of exposure to the standardized fire. The 20 mm thickness improves the degree of protection in the order

29.4, 32.8, 24.4, 19.8, 17 and 15.5% at the same times. At a thickness of 30 mm, the degree of protection improves and reaches 42.1, 44.0, 37.1, 30.4, 26.1 and 23.3% at the same ISO 834 times.

For the beam without thermal protection, the maximum concrete temperature reached 683.2 °C. When protected with 10, 20, and 30 mm layers of M4 mortar, these maximum temperatures were reduced to 349.9, 198.2, and 134.6 °C, respectively. Similarly, with M18 mortar, maximum temperatures of 416.2, 272.6, and 189.1 °C were observed for the same thicknesses. In contrast, the use of M7 or M22 mortars resulted in significantly higher maximum temperatures of 631.0 °C, 577.5 °C, and 523.7 °C, respectively.

These results highlight not only the effectiveness of thermal protection in reducing temperature but also the significant influence of mortar thermal properties on heat transfer. Mortars with lower thermal conductivity and diffusivity, combined with higher specific heat capacity, provide enhanced insulation by slowing heat penetration and increasing the energy required to raise the temperature of the concrete substrate. Therefore, the differences in maximum temperatures can be directly correlated to the intrinsic thermal conductivity, diffusivity, and specific heat capacity of each mortar type, underscoring the importance of selecting mortars with favorable thermal properties for fire protection in structural applications.

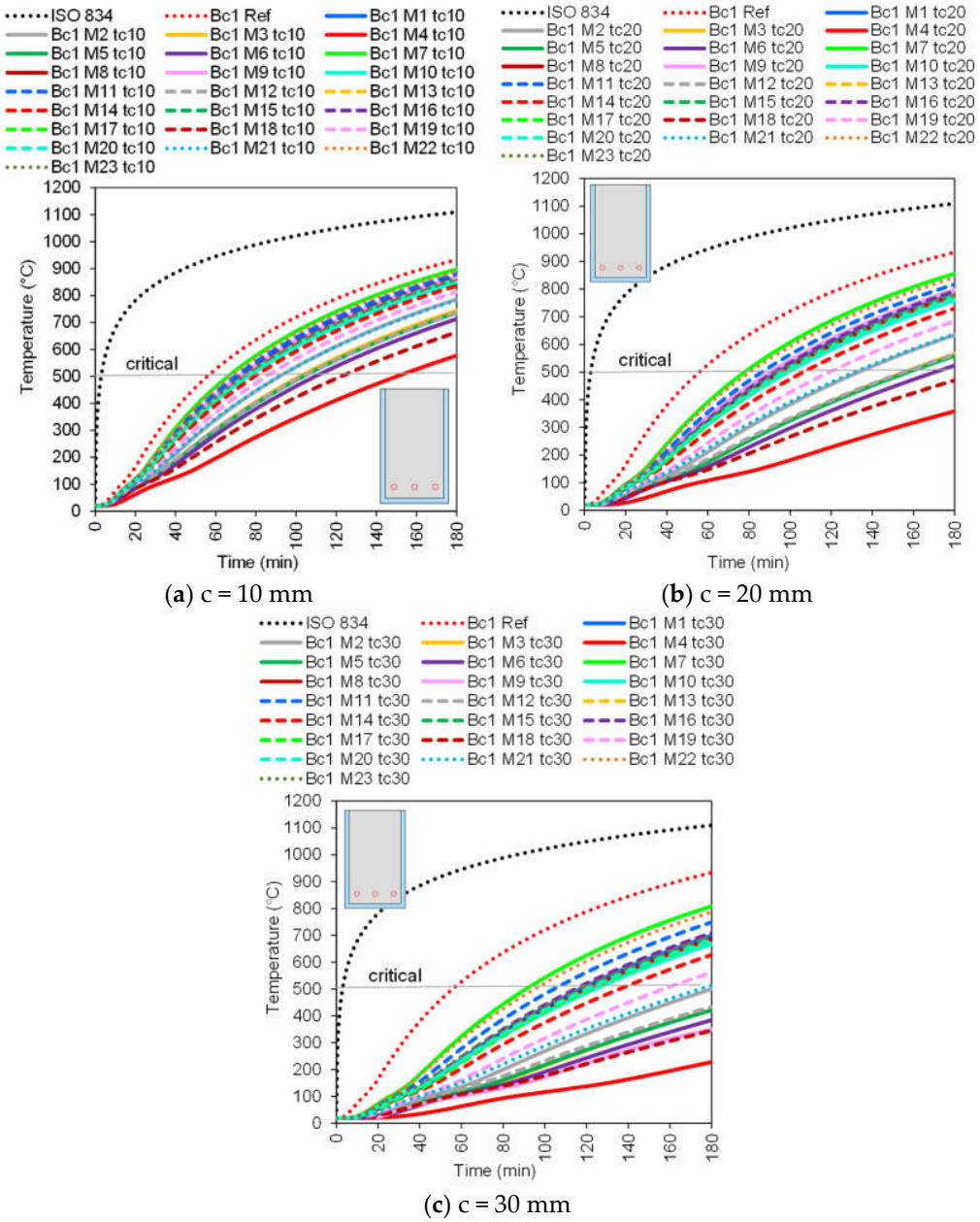
3.3.2. Average Temperature in the Reinforcements

The average temperature of the reinforcements is shown in the Figure 8a–c for mortar thickness 10 to 30 mm, respectively.

In RC structures exposed to fire, the reinforcement is the part most sensitive to high temperatures. In fact, all mortars lower the average temperature and, depending on the thickness and composition of the mortar, can prevent the reinforcement from reaching its critical temperature. It can be stated in all cases that M4 and M18 are the most effective and have the best thermal behavior, the M4 being the most effective of all cases.

Assuming that the thickness of M4 is 10 mm, a maximum temperature of 577.1 °C was reached at the end of the test, with the temperature decreasing in the order 64.5, 62.1, 54.3, 47.8, 42.6 and 38.2% after 30, 60, 90, 120, 150 and 180 min of standardized fire compared to the reference beam. When the thickness is increased to 20 mm, the reduction in average temperature improves to 83.0, 78.9, 76.0, 70.4, 65.4 and 61.6% for the same fire times, and the maximum temperature to which the rebars are exposed is 228.2 °C. When the thickness is increased to 30 mm, the average temperature decreases to 91.0, 87.4, 84.2, 82.2, 79.0 and 75.5%, and the maximum temperature of the rebars at the end of the analysis is 228.2 °C. As can be seen, the reduction in average temperature can be almost 100%, which underlines the effectiveness of this type of mortar.

M18 also performed well in fire. The maximum temperature to which the rebars were exposed at mortar thicknesses of 10, 20 and 30 mm was 663.6, 470.6 and 344.4 °C, respectively. On the other hand, M7 and M22 showing the worst behavior, subjected the rebars to a temperature in order of 897.6, 856.4 and 808.5 °C at the end of the test.



(**a**) c = 10 mm (**b**) c = 20 mm

(**c**) c = 30 mm

Figure 8. Cross-section temperature in the reinforcements in the case of Bc1 beams.

3.4. Bc2 Beams

3.4.1. Average Temperature in the Concrete

The average temperature of the concrete part of the cross-section is shown in the Figure 9a–c for mortar thickness 10 to 30 mm, respectively.

Regarding the performance of the Bc2 beams with 10 mm thick mortars, the M4 mortar was the one that showed the best thermal protection in the beam. In this case, the temperature reduction in the cross-section of the RC beam without thermal protection (Ref) was 70.7, 73.8, 75.2, 74.9, 73.7 and 71.8% lower (at 30, 60, 90, 120, 150 and 180 min of standardized fire exposure, respectively). At a protective thickness of 20 mm, the M4 mortar also showed the best performance among all other mortars by reducing the average temperature of the beam cross-section between 79.9 and 83.0%. When the thickness of the coating was increased to 30 mm, the degree of protection reached a maximum of 88.6% compared to the reference case (i.e., RC beams without thermal barrier).

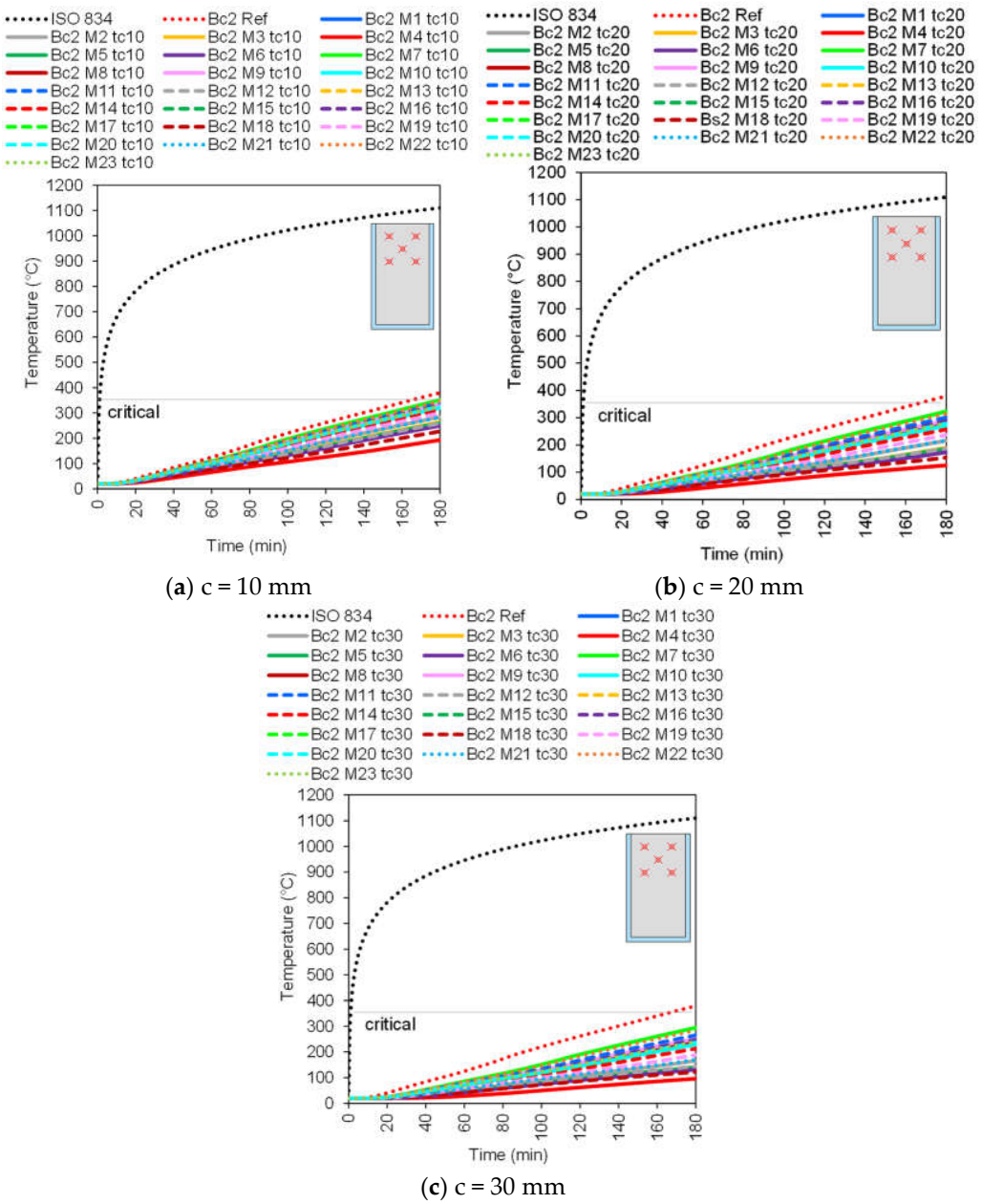


Figure 9. Cross-section temperature in the concrete part in the case of Bc2 beams.

M18 was the second mortar that showed the best thermal performance. With a mortar thickness of 10 mm, the reduction in the average temperature (without thermal protection, named as "ref") of the cross-section was between 65.5 and 71.5% (depending on the time considered). When the thickness is increased to 20 and 30 mm, the average cross-section temperature reduces by 75.0 to 78.5 % and 79.8 to 83.6% respectively.

Case M6 showed similar results to M18 and can be considered approximately equivalent to M18 in terms of thermal performance as a thermal barrier for reinforced concrete structures. Compared to the beam without mortar ("ref"), the temperature field in the cross-section is reduced by 63.5 to 69.7% (depending on the considered time of ISO 834 standardized fire). If the thickness is increased to 20 and 30 mm, the reduction in the cross-section temperature reaches 75.1 to 77.6 % and 81.3 to 83.3% respectively.

Among the mortars that performed worse, M7 and M22 showed similar performance and can be considered equivalent when used as thermal mortars to protect reinforced concrete structures in case of fire. On average, at mortar thicknesses of 10, 20 and 30 mm, both

mortars showed a reduction in cross-sectional temperature of 55, 60 and 65, respectively, compared to a reinforced concrete beam without thermal protection.

In this case, due to the cross-sectional dimensions of the beam, it is important to emphasize that all mortars do not raise the average temperature of the concrete part above the critical. Only the beam without thermal mortar reaches the critical temperature, but in a very short period of time and with a very reduced temperature, which can be assumed to be controllable (i.e., negligible). In view of the concrete part of the cross-section, the use of mortar is not necessary. In fact, for RC beams, the use of mortar is usually necessary to protect the reinforcement from the critical temperature, as demonstrate in the next section.

3.4.2. Average Temperature in the Reinforcements

The average temperature of the reinforcements is shown in the Figure 10a–c for mortar thickness 10 to 30 mm, respectively.

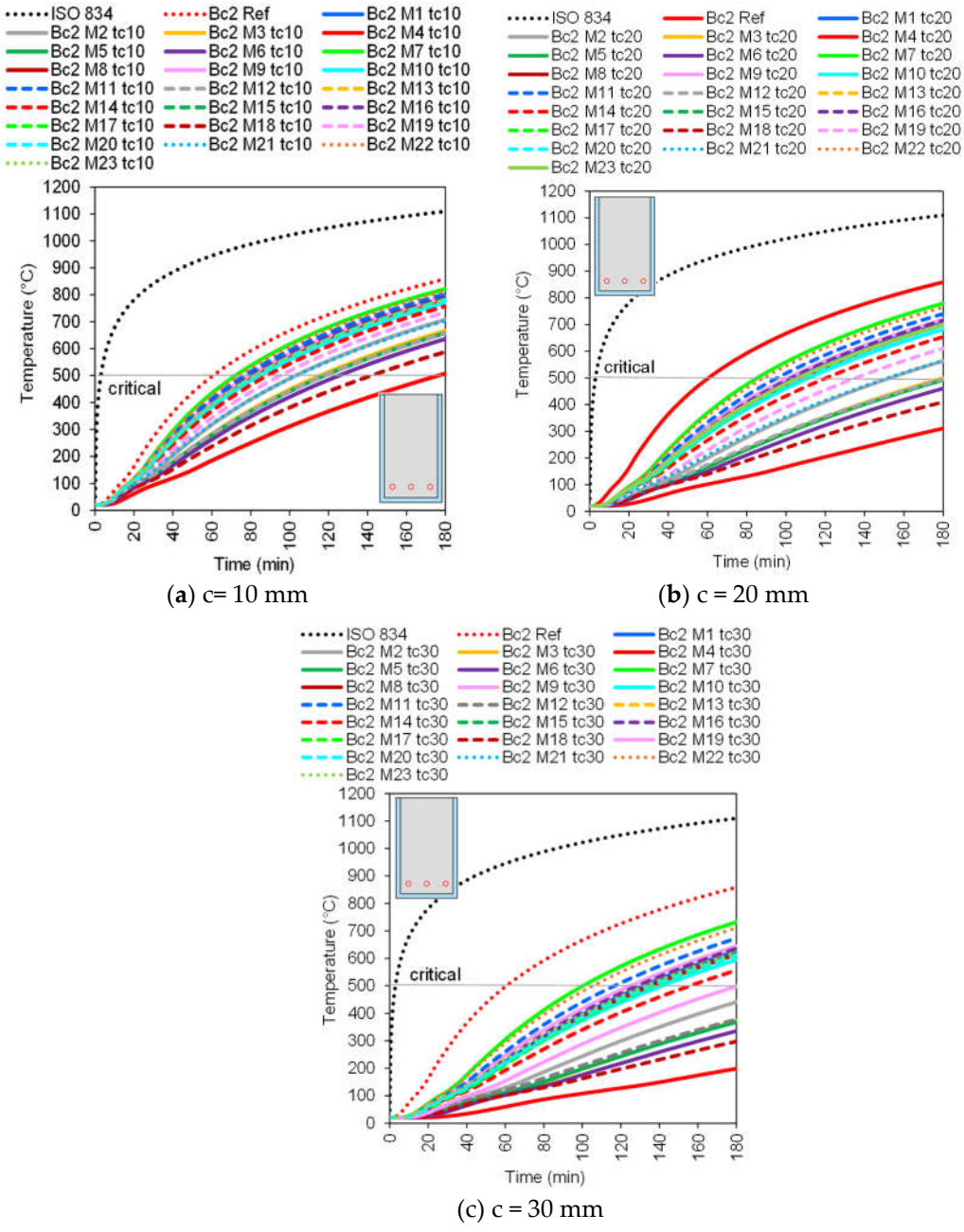


Figure 10. Cross-section temperature in the reinforcements in the case of Bc2 beams.

The temperature in the reinforcement causes more critical damage to the bending capacity of the beams and is more important to justify the mechanical capacity of these structures. It is important to emphasize that there are cases in which the mortar protects the beams – and therefore the reinforcement – from reaching the critical temperature, but in some cases the mortar does not generate an interesting thermal performance. The nature of the mortar is then a fundamental criterion to be taken into account in the structural design when additional protection must be considered.

As mentioned above, the M4 mortar shows the best thermal performance when it comes to temperature in concrete and is the most efficient solution to protect RC structures, regardless of thickness. Compared to the beam without mortar (ref), the temperature of the rebars with an M4 coating of 10 mm thickness is reduced by 65.5, 61.9, 55.1, 49.3, 44.6 and 40.9 in 30, 60, 90, 120, 150 and 180 min, respectively, according to ISO 834. If the thickness is increased to 20 mm, the reduction improves and is 83.2, 78.9, 75.9, 71.3, 67.1 and 63.8 lower compared to the "ref" beam at 30, 60, 90, 120, 150 and 180 min ISO 834 exposure respectively. When improving to 30 mm, the reduction reaches 90.9, 87.4, 84.2, 82.1, 79.5 and 76.8 at 30, 60, 90, 120, 150 and 180 min ISO 834 exposure.

M18 and M6 again show similar behavior and can be considered equivalent in terms of the thermal behavior and protection of these structures. As already observed with M4, the effectiveness of the thermal protection of the mortars decreases with increasing duration and temperature of the fire. In the first 30 min, the reduction in temperature of the reinforcements (compared to the reference beam) is around 56.0% in both cases and decreases to 27.0% at the end of the fire (180 min) with a mortar thickness of 10 mm. If the mortar thickness is increased to 20 mm, the temperature reduction in the first 30 min is around 72.0% and 50.0% at the end of the fire program. With an increase to 30 mm, the reduction is 84.0% in the first 30 min and decrease to 63.0% at the end of the test (180 min).

On the other hand, M7 and M22 show the worst behavior and do not protect the reinforcement from reaching the critical temperature. Assuming that the mortar is 10 mm thick, the average temperature (with respect to the reference beam) decreases by 25.0, 12.0, 9.0, 7.0, 6.0 and 5.0% at 30, 60, 90, 120, 150 and 180 min of fire exposure according to ISO 834. If the thickness is increased to 20 mm, the temperature reduction is about 44.0, 28.0, 19.0, 15.0, 12.0 and 11.0% at 30, 60, 90, 120, 150 and 180 min. At a thickness of 30 mm, the temperature reduction was 57.0, 41.0, 29.0, 23.0, 19.0 and 17.0% at 30, 60, 90, 120, 150 and 180 min of standardized fire exposure.

In all cases of mortar thickness, the M4 coating is the only mortar that protects the reinforcement from reaching a critical temperature.

4. Cross-Sectional Temperature Field

Some temperature fields of the cross-sections are shown in Figures 11 and 12 for steel and reinforced concrete structures, respectively. The temperature field is intended to provide information on how the temperature of the external fire is distributed in the cross-section of the structures and cross-sections considered in the numerical analysis. It can be seen that due to the high thermal diffusivity in the cross-section of steel structures, the temperature field is more uniform over the entire cross-section than in concrete, where the temperature field is not uniform.

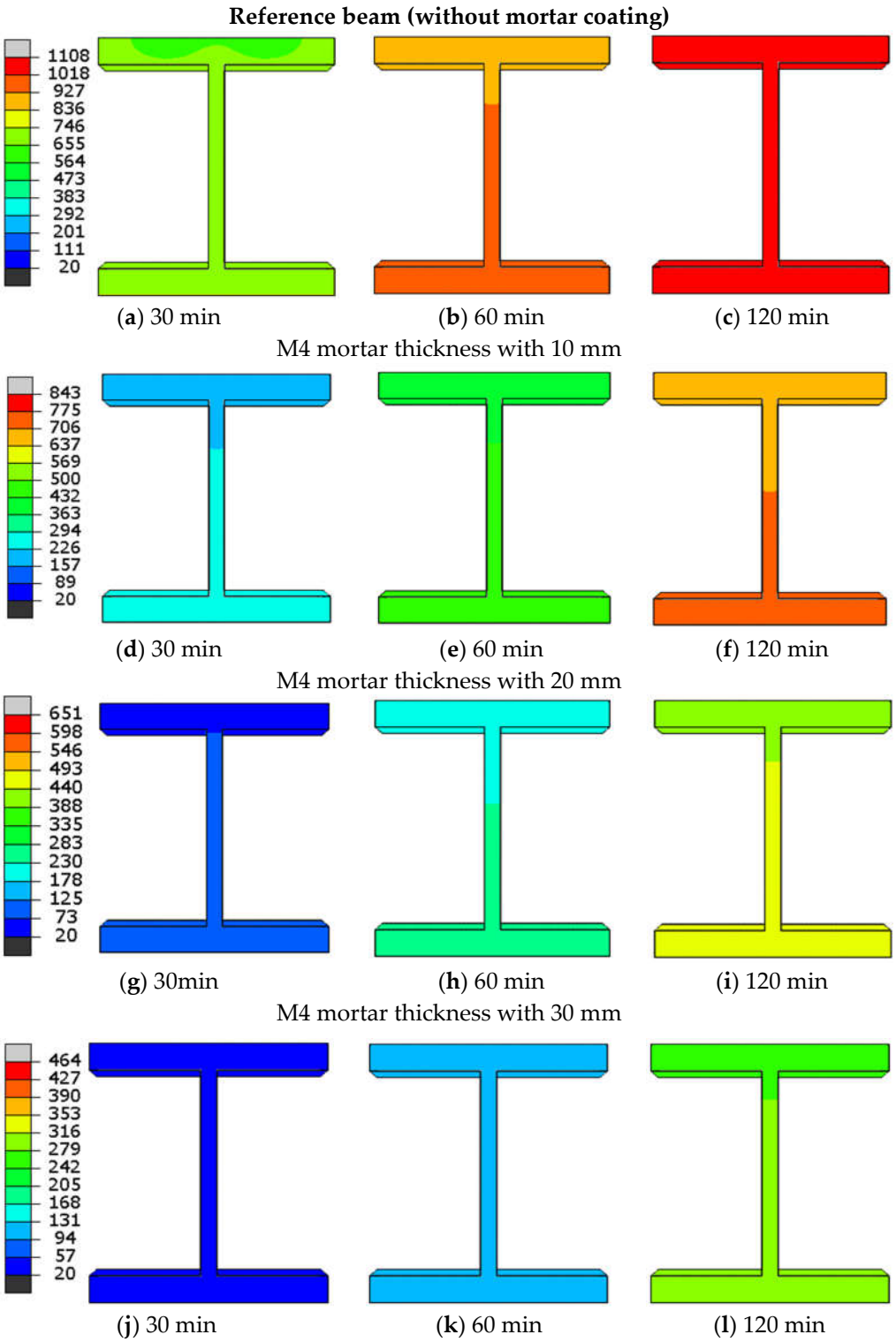


Figure 11. Temperature field in steel structures cross-section at different ISO 834 fire times (temperature in °C).

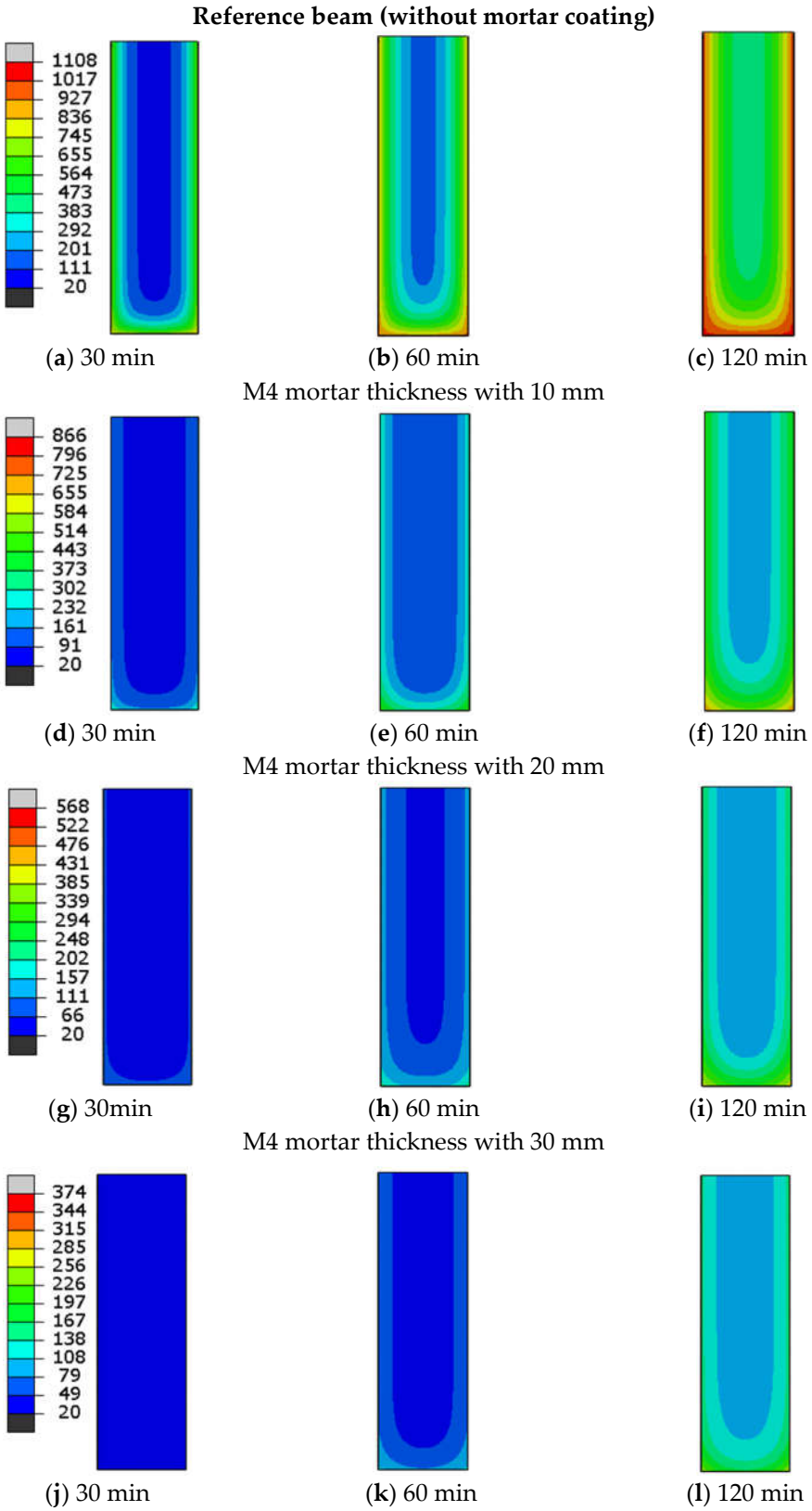


Figure 12. Temperature field in reinforced concrete structures cross-section at different ISO 834 fire times (temperature in °C).

5. Critical Discussion of Results

The M4 mortar, with using 40% Glass Fiber Reinforced Polymers Powder Slag replacement, shows the best results and can reduce the average cross-section temperature in the

structures by almost 100%. Recent experimental investigations can help the authors to justify the numerical results proposed in this study. Thermogravimetric analysis (TGA) shows that the decomposition of the epoxy resin matrix in the GFRP powder occurs primarily between 300 and 450 °C, with a mass loss of about 55% at 450 °C. The remaining 45% consists of heat-resistant glass fibers and pyrolytic carbon, which underlines the high thermal stability of the material [22].

In the context of fire protection, GFRP powder has been utilized in lightweight geopolymer mortars. Studies show that incorporating GFRP powder can influence the thermal conductivity of these mortars, with variations depending on the specific mix and additives used. However, the overall thermal insulation properties are also significantly affected by other components such as foaming agents and vitrified micro bubbles [23]. GFRP powder demonstrates commendable thermal stability due to the heat-resistant nature of its glass fibers. While it exhibits limited pozzolanic reactivity, its incorporation into composite materials can impact the thermal properties, especially when combined with other additives. Continued research is essential to optimize its use in applications requiring enhanced thermal performance [22].

In fact, GFRP powder, derived from recycled glass fiber-reinforced plastics, contributes to the thermal resilience of mortars through its inherent properties. The glass fibers possess low thermal conductivity and high melting points, which impede heat transfer and delay the onset of structural weakening. Furthermore, the polymer matrix within GFRP powder, even after partial decomposition, creates a porous microstructure that enhances the material's insulating capabilities. Studies have shown that incorporating GFRP powder into mortars can lead to significant reductions in thermal conductivity, thereby improving fire resistance.

M18, a mortar with expanded perlite with relace sand in 100%, also shows very good results and is the second mortar with the best thermal behavior. According to the literature, the addition of expanded perlite to mortars or concretes mixes significantly reduces thermal conductivity due to its porous structure, which traps air and hinders heat transfer. Studies have shown that replacing natural sand with expanded perlite can lead to a significant reduction in thermal conductivity. For example, Oktay et al. [24] reported a reduction in thermal conductivity of 22.96 to 81.48% when 10 to 50% of the sand was replaced with perlite particles ranging in size from 0.15 to 11 mm. Similarly, studies by Demirboğa and Gül [25] showed a reduction in thermal conductivity of 23% with a perlite content of 30% and a reduction of 10% when fly ash was also added to the mixture.

M6 was the third mortar with the best results can be highlighted as a material that can reduce the temperature range in the cross section of the structures. A mortar formulation comprising 40% Glass Fiber Reinforced Polymer (GFRP) powder and 20% fly ash as cement replacements demonstrates superior thermal performance when exposed to fire. This enhanced fire resistance is attributed to the synergistic effects of GFRP powder's insulating properties and fly ash's pozzolanic reactivity, which together mitigate heat transfer and structural degradation during high-temperature events.

Fly ash, a by-product of coal combustion, is used as a partial substitute for cement in the mortar mix. Its pozzolanic properties facilitate the formation of additional calcium silicate hydrate gel (C–S–H) during the reaction with calcium hydroxide, resulting in a denser and more durable microstructure. This compaction reduces the permeability of the mortar, limiting the penetration of heat and moisture during fire exposure. Research shows that mortars modified with fly ash have better thermal stability and resistance to high temperatures compared to conventional cement-based mortars. For example, a study by Öztürk (2022) [26] showed that mortars containing 15% fly ash had better compressive strength at 400 and 800 °C than control samples without fly ash. This enhanced fire

resistance is attributed to the ceramic-like characteristics of the geopolymer, which provide better thermal stability and structural integrity under elevated temperatures.

Regarding the M7 (Raw Vermiculite 30% sand replacement) and M22 (lightweight aggregates of Expanded Polyvinyl Chloride 15% sand replacement) cases, their thermal protection was minimal compared to the other cases.

Despite vermiculite's reputation as a thermal insulator, mortars containing large amounts—around 30%—of raw vermiculite as a sand substitute can exhibit poor thermal behavior when exposed to fire. This paradox is due to the high porosity, low density and weak interaction of the material with the cement matrix. While the expanded structure of vermiculite can reduce thermal conductivity, excessive replacement disrupts the integrity of the mix, leading to increased permeability and micro-cracking under thermal stress. These defects act as heat paths and allow rapid temperature propagation in the mortar. In addition, the lamellar morphology of vermiculite leads to poor bonding with the surrounding paste, which reduces cohesion and increases susceptibility to thermal shrinkage and spalling. Studies such as that by Demirboğa and Gül (2003) [25] have shown that high-volume lightweight aggregates compromise the mechanical strength and fire resistance of mortars due to these microstructural weaknesses. Similarly, Sarkar and Bose (2016) [27] reported lower fire resistance of concretes with vermiculite due to weak matrix-aggregate interaction. Although vermiculite has insulating value at lower dosages, the use of 30% raw vermiculite as a sand substitute undermines both structural stability and fire resistance, making it unsuitable for high performance fire protection applications without further modification.

Mortars containing expanded polyvinyl chloride (PVC) as a lightweight aggregate for the partial replacement of sand—e.g., with a proportion of 15%—generally have a low thermal performance in the event of fire. This is primarily due to the thermal instability and combustibility of PVC polymers, which begin to decompose at temperatures of 140–200 °C. When exposed to heat, PVC becomes dehydrated. When exposed to heat, PVC is dehydrochlorinated, releasing hydrogen chloride (HCl) gas and leaving carbonaceous residues that do not contribute to structural integrity [28]. When the PVC burns or melts, internal voids and microcracks are created, which severely affect the cement matrix and increase porosity and thermal conductivity. These microstructural defects facilitate heat transfer and reduce the effectiveness of the mortar as a thermal barrier. In addition, the loss of bonding between the PVC particles and the cement paste reduces mechanical cohesion, which increases the risk of cracking, spalling and structural collapse at high temperatures. The resulting combustion also produces dense, toxic smoke, which increases the risk of fire [29]. Although PVC-based aggregates can lead to a reduction in density under ambient conditions, they are not suitable for fire protection applications in cementitious composites due to their poor thermal resistance and degradation behavior.

As a suggestion for future research, the authors encourage conducting a coupled thermomechanical analysis based on the results presented in this study, including the use of different fire exposure curves. This approach would enhance the understanding of structural performance under fire conditions, as demonstrated in previous research published by the lead authors of this study [30–32].

6. Conclusions

The study evaluated 23 different mortar types, each with different composition and additives. It was found that all mortar types contributed to reducing the internal temperature of structural elements, such as steel and reinforced concrete, during fire exposure. The performance varied based on the coating thickness and specific thermal properties of the mortars used. The main conclusion of the paper is:

(1). Mortars containing glass fiber reinforced polymer (GFRP) as a slag substitute and those incorporating expanded perlite as a sand replacement demonstrated the highest thermal insulation capacity. These mixtures achieved temperature reductions of up to nearly 100% compared to unprotected elements, confirming their superior effectiveness in fire resistance applications.

(2). In contrast, mortars modified with 30% vermiculite or 15% lightweight expanded polyvinyl chloride (PVC) as sand substitutes exhibited the lowest thermal performance, with significantly higher internal temperatures. These results underscore the critical role of material selection in achieving effective thermal protection.

(3). The findings highlight the influence of specific additives on thermal conductivity and overall heat transfer. GFRP powder enhances thermal stability due to the presence of heat-resistant glass fibers, while expanded perlite improves insulation through its highly porous structure, which limits thermal conductivity.

(4). The specific heat was identified as a gap in all the experimental studies reviewed in the literature. Therefore, it is recommended that future experimental research include the measurement of specific heat when conducting thermal analyses of these mortars.

Author Contributions: Conceptualization, F.L.B. and A.S.H.; methodology, F.L.B. and A.S.H.; software, F.L.B.; validation, F.L.B., D.B.S., E.C.P.; formal analysis, F.L.B., D.B.S., E.C.P.; investigation, F.L.B. and A.S.H.; data curation, F.L.B. and A.S.H.; writing—original draft preparation, F.L.B.; writing—review and editing, F.L.B., A.S.H., D.B.S., E.C.P.; visualization, F.L.B.; supervision, F.L.B.; project administration, F.L.B. All authors have read and agreed to the published version of the manuscript.

Funding: This research received no external funding.

Institutional Review Board Statement: Not applicable.

Informed Consent Statement: Not applicable.

Data Availability Statement: Data are contained within the article.

Conflicts of Interest: The authors declare no conflicts of interest.

Appendix A

In this Appendix A, the mixture of the proposed mortar described in Table 1 is presented.

Mortar Name	Cement (Kg/m^3)	Fayalite Slag (Kg/m^3)	Blast Furnace Slag (Kg/m^3)	Ladle Slag (Kg/m^3)	Fly Ash (Kg/m^3)	Slag (Kg/m^3)	Sand (Kg/m^3)	RV (Kg/m^3)	PCM impregnated sepiolite (Kg/m^3)	RCB (Kg/m^3)	OSW (Kg/m^3)	FSA (Kg/m^3)	MPCM (Kg/m^3)	GFRP (Kg/m^3)	EP (Kg/m^3)	RP (Kg/m^3)	VSS (Kg/m^3)	EPVC (Kg/m^3)	Water (Kg/m^3)	SH (Kg/m^3)	SS (Kg/m^3)	w/b	Alkali activator (ml)	NA+ (Kg/m^3)	SP (%)
M1	480	-	-	-	-	-	1440	-	-	-	-	-	-	-	-	-	-	-	288	-	-	0.6	-	-	-
M2	384	-	-	-	76.8	-	1440	-	-	-	-	-	-	19.2	-	-	-	-	276	-	-	0.6	150	-	-
M3	-	-	-	-	76.8	384	1440	-	-	-	-	-	-	19.2	-	-	-	-	230	-	-	0.5	150	-	-
M4	-	-	-	-	-	288	1440	-	-	-	-	-	-	192	-	-	-	-	173	-	-	0.6	150	-	-
M5	288	-	-	-	-	-	1440	-	-	-	-	-	-	192	-	-	-	-	173	-	-	0.6	-	-	-
M6	230	-	-	-	57.6	-	1440	-	-	-	-	-	-	192	-	-	-	-	173	-	-	0.6	-	-	-
M7	520 *	-	-	-	-	-	1138 **	650	-	-	-	-	-	-	-	-	-	-	260	-	-	0.5	-	-	-
M8	520 *	-	-	-	-	-	-	193	-	-	-	-	-	-	-	-	-	-	260	-	-	0.5	-	-	-
M9	750	-	-	-	-	-	1080	-	270	-	-	-	-	-	-	-	-	-	550	-	-	0.7	-	-	-
M10	750	-	-	-	-	-	810	-	540	-	-	-	-	-	-	-	-	-	900	-	-	1.2	-	-	-
M11	520	-	-	-	-	-	1138	-	-	197	-	-	-	-	-	-	-	-	260	-	-	0.5	-	-	-
M12	520	-	-	-	-	-	-	-	-	657	-	-	-	-	-	-	-	-	260	-	-	0.5	-	-	-
M13	450	-	-	-	-	-	1282	-	-	-	68	-	-	-	-	-	-	-	258	-	-	0.6	-	-	-
M14	450	-	-	-	-	-	1147	-	-	-	203	-	-	-	-	-	-	-	325	-	-	0.7	-	-	-
M15	645	-	-	-	-	-	1290	-	-	-	-	-	129	-	-	-	-	-	355	-	-	0.6	-	-	-
M16	488.8	-	-	-	-	-	1466.6	-	-	-	-	-	97.6	-	-	-	-	-	298	-	-	0.6	-	-	-
M17	389.8	-	-	-	-	-	1559.2	-	-	-	-	-	77.9	-	-	-	-	-	265	-	-	0.7	-	-	-
M18	-	-	-	-	450	-	-	-	-	-	-	-	-	-	-	-	-	-	130	-	-	0.3	-	45	-
M19	-	-	-	-	450	-	-	-	-	-	-	-	-	-	100	-	-	-	130	-	-	0.3	-	45	-
M20	500	-	-	-	-	-	950	-	-	-	-	-	-	-	-	-	50	-	250	-	-	0.5	-	-	-
M21	500	-	-	-	-	-	800	-	-	-	-	-	-	-	-	-	200	-	250	-	-	0.5	-	-	-
M22	450	-	-	-	-	-	1148 ***	-	-	-	-	-	-	-	-	-	-	26.9	225	-	-	0.5	-	-	0.9
M23	450	-	-	-	-	-	337.5 ***	-	-	-	-	-	-	-	-	-	-	134.7	225	-	-	0.5	-	-	0.45

* CSA cement; ** Silica Sand; *** 60% quarry sand and 40% sea sand.

References

1. *ISO 23932*; Fire Safety Engineering—General Principles. International Organization for Standardization: Geneva, Switzerland, 2018; Volume 1, pp. 1–26.
2. *ISO 834*; Fire-Resistance Tests—Elements of Building Construction. International Organization for Standardization: Geneva, Switzerland, 1999; Volume 1, pp. 1–25.
3. Rong, X.; Xu, W.; Zhang, T.; Zhang, J. Mechanical and thermal properties of insulated mortar incorporated with GFRP powder. *Constr. Build. Mater.* **2024**, *416*, 135259. [CrossRef]
4. Tchekwagep, J.J.K.; Yang, F.; Wang, S.; Zhao, P.; Huang, S.; Yang, C.; Cheng, X. Chinese raw vermiculite: A potential additive for improving the thermal properties of calcium sulfoaluminate cement-blended mortars for applications in hot regions. *J. Build. Eng.* **2024**, *92*, 109723. [CrossRef]
5. Topçu, İ.B.; Bayram, M.; Ustaoğlu, A.; Hekimoğlu, G.; Erdoğmuş, E.; Sarı, A.; Gencel, O.; Ozbakkaloglu, T. Innovative cementitious mortar incorporated with sepiolite based shape-stable phase change material for thermal controlling of buildings. *Constr. Build. Mater.* **2024**, *426*, 136124. [CrossRef]
6. Zhao, J.; Huang, G.; Guo, Y.; Gupta, R.; Liu, W.V. Developing thermal insulation cement-based mortars using recycled carbon black derived from scrapped off-the-road tires. *Constr. Build. Mater.* **2023**, *393*, 132043. [CrossRef]
7. EL boukhari, M.; Merroun, O.; Maalouf, C.; Bogard, F.; Kissi, B. Enhancing mechanical and thermal properties of sustainable cement mortar through incorporation of olive solid waste aggregates. *Mater. Today Proc.* **2023**. [CrossRef]
8. Adediran, A.; Yliniemi, J.; Moukannaa, S.; Ramteke, D.; Perumal, P.; Illikainen, M. Enhancing the thermal stability of alkali-activated Fe-rich fayalite slag-based mortars by incorporating ladle and blast furnace slags: Physical, mechanical and structural changes. *Cem. Concr. Res.* **2023**, *166*, 107098. [CrossRef]
9. Asadi, I.; Ji, G.; Steiner, G. Impact of microencapsulated phase change materials (PCMs) on the thermal and mechanical performance of cement mortar. *Dev. Built Environ.* **2025**, *21*, 100594. [CrossRef]
10. Karakaş, H.; İlKentapar, S.; Durak, U.; Örklemez, E.; Özuzun, S.; Karahan, O.; Atiş, C.D. Properties of fly ash-based lightweight-geopolymer mortars containing perlite aggregates: Mechanical, microstructure, and thermal conductivity coefficient. *Constr. Build. Mater.* **2023**, *362*, 129717. [CrossRef]
11. Salem, T.; Fois, M.; Omikrine-Metalssi, O.; Manuel, R.; Fen-Chong, T. Thermal and mechanical performances of cement-based mortars reinforced with vegetable synthetic sponge wastes and silica fume. *Constr. Build. Mater.* **2020**, *264*, 120213. [CrossRef]
12. Latroch, N.; Benosman, A.S.; Bouhamou, N.E.; Senhadji, Y.; Mouli, M. Physico-mechanical and thermal properties of composite mortars containing lightweight aggregates of expanded polyvinyl chloride. *Constr. Build. Mater.* **2018**, *175*, 77–87. [CrossRef]
13. Abaqus Abaqus Analysis User's Guide. 2016, Simulia. Available online: https://www.3ds.com/products/simulia/abaqus (accessed on 1 June 2025).
14. *EN 1992-1.2*; Eurocode 2: Design of Concrete Structures—Part 1-2: General Rules—Structural Fire Design. European Committee for Standardization: Brussels, Belgium, 2004.
15. Banerji, S.; Kodur, V. Numerical model for tracing the response of Ultra-High performance concrete beams exposed to fire. *Fire Mater.* **2023**, *47*, 322–340. [CrossRef]
16. *ASTM E 119*; Standard Test Methods for Fire Tests of Building Construction and Materials. ASTM International: Geneva, Switzerland, 2018.
17. Bolina, F.L.; Schallenberger, M.; Carvalho, H. Experimental and numerical evaluation of RC ribbed slabs in fire conditions. *Structures* **2023**, *51*, 747–759. [CrossRef]
18. Bolina, F.L.; Poleto, G.; Carvalho, H. Proposition of parametric data for UHPC at high temperatures. *J. Build. Eng.* **2023**, *76*, 107222. [CrossRef]
19. Bolina, F.L.; Rodrigues, J.P.C. Finite element analysis criteria for composite steel decking concrete slabs subjected to fire. *Fire Saf. J.* **2023**, *139*, 103818. [CrossRef]
20. Kodur, V.K.R.; Phan, L. Critical factors governing the fire performance of high strength concrete systems. *Fire Saf. J.* **2007**, *42*, 482–488. [CrossRef]
21. Yeo, H.; Cho, K.S.; Cho, B.Y.; An, J.H.; Kim, H.J. A Study on Relations Between Section Shape Factor and Temperature History of Steel of Composite Beam Subjected to Standard Fire under Same Thickness Condition of Spray-Type Fire Resistant Materials. *Adv. Mat. Res.* **2013**, *671–674*, 912–920. [CrossRef]
22. Shaoqing, L.; Lik-ho, T.; Hongqiang, M.; Jianping, G.; Chao, W. Pozzolanic Analysis of GFRP Powder from Retired Wind Turbine Blades as Supplementary Cementitious Material. *J. Mater. Civ. Eng.* **2025**, *37*, 04024543. [CrossRef]
23. Zhang, M.; Qiu, X.; Shen, S.; Wang, L.; Zang, Y. Mechanical and Thermal Insulation Properties of rGFRP Fiber-Reinforced Lightweight Fly-Ash-Slag-Based Geopolymer Mortar. *Sustainability* **2023**, *15*, 7200. [CrossRef]
24. Oktay, H.; Yumrutaş, R.; Akpolat, A. Mechanical and thermophysical properties of lightweight aggregate concretes. *Constr. Build. Mater.* **2015**, *96*, 217–225. [CrossRef]

25. Demirboğa, R.; Gül, R. The effects of expanded perlite aggregate, silica fume and fly ash on the thermal conductivity of lightweight concrete. *Cem. Concr. Res.* **2003**, *33*, 723–727. [CrossRef]
26. Öztürk, M. Elevated Temperature Resistance of Mortars Including Ground Granulated Blast Furnace Slag, Fly ash and Silica Fume. *Osman. Korkut Ata Üniv. Fen Bilim. Enst. Derg.* **2022**, *5*, 143–153. [CrossRef]
27. Sarkar, A.; Bose, S. Exploring impact of opaque building envelope components on thermal and energy performance of houses in lower western Himalayans for optimal selection. *J. Build. Eng.* **2016**, *7*, 170–182. [CrossRef]
28. Al-Salem, S.M.; Lettieri, P.; Baeyens, J. Recycling and recovery routes of plastic solid waste (PSW): A review. *Waste Manag.* **2009**, *29*, 2625–2643. [CrossRef] [PubMed]
29. Albite-Ortega, J.; Sánchez-Valdes, S.; Ramírez-Vargas, E.; Medellín-Rodríguez, F.J.; Devalle, L.F.R.; Rodriguez-Fernandez, O.S.; Rivera-Salinas, J.E.; Martínez-Colunga, J.G.; Da-Silva, L.; Morales-Cepeda, A.B.; et al. Influence of ammonium polyphosphate-modified polypropylene on flammability characteristics of polypropylene keratin and chitosan sustainable composites. *Fire Mater.* **2023**, *47*, 170–181. [CrossRef]
30. Bolina, F.L.; Henn, A.S. Eco-Friendly Reinforced Concrete Beams Exposed to Standardized Fire: A Thermal Finite Element Analysis. *Sustainability* **2025**, *17*, 2951. [CrossRef]
31. Bolina, F.L.; Fachinelli, E.G.; Rodrigues, J.P.C. Analysis of building structures subjected to electric vehicle fires. *J. Build. Eng.* **2025**, *107*, 112769. [CrossRef]
32. Bolina, F.L.; Henn, A.S.; Lago, B.D. Simplified Design Procedure for RC Ribbed Slabs in Fire Based on Experimental and Numerical Thermal Analysis. *Buildings* **2025**, *15*, 1631. [CrossRef]

Disclaimer/Publisher's Note: The statements, opinions and data contained in all publications are solely those of the individual author(s) and contributor(s) and not of MDPI and/or the editor(s). MDPI and/or the editor(s) disclaim responsibility for any injury to people or property resulting from any ideas, methods, instructions or products referred to in the content.